

A study of long bone fractures via reconstruction of pedestrian accident using Multi-body system and Lower Extremity FE model

Bingyu Wang^{*}, Jikuang Yang^{**}, Otte Dietmar^{***}

^{*} Research Center of Vehicle and Traffic Safety (VTS), State key Laboratory of Advanced Design Manufacturing for Vehicle Body, Hunan University, Changsha, 410082, China

^{**} Department of Applied Mechanics, Chalmers University of Technology, Gothenburg 41296, Sweden

^{***} Accident Research Unit, Medical University of Hannover, Hannover, 30625, Germany

Abstract: This study aimed at prediction of long bone fractures and assessment of lower extremity injury mechanisms in real world passenger car to pedestrian collision. For this purpose, two pedestrian accident cases with detail recorded lower limb injuries were reconstructed via combining MBS (Multi-body system) and FE (Finite element) methods. The code of PC Crash was used to determine the boundary conditions before collision, and then MBS models were used to reproduce the pedestrian kinematics and injuries during crash. Furthermore, a validated lower limb FE model was chosen to conduct reconstruction of injuries and prediction of long bone fracture via physical parameters of von Mises stress and bending moment. The injury outcomes from simulations were compared with hospital recorded injury data and the same long bone fracture patterns and positions can be observed. Moreover, the calculated long bone fracture tolerance corresponded to the outcome from cadaver tests. The result shows that FE model is capable to reproduce the dynamic injury process and is an effective tool to predict the risk of long bone fractures.

Key words: lower extremity FE model, long bone fracture, pedestrian accident, injury reconstruction

1 INTRODUCTION

As vulnerable road users, pedestrians are injured frequently in vehicle accident due to lack of outer protective equipments. Every year a lot of unprotected pedestrians are injured or died in road traffic accidents. According to the report of 2010, in European Commission, 6004 pedestrians were killed, accounted for 20% of all fatalities in the traffic accident^[1]. Statistic analysis of traffic accidents indicated that lower extremity is the most frequently injured body region, accounting for 32.8% of all injuries^[2]. Although rarely fatal with an AIS (Abbreviated Injury Scale) rating ranging from 1 to 3, lower limb injuries will cause long-term impairment and even disability, resulting huge social and economical cost^[3]. As one of the most common injury modes in car-pedestrian crashes, long bone fracture is mainly attributed to the excessive bending moment caused from the contact between lower limb and car front end structure^[4]. The statistical data showed that bumper and bonnet leading edge were the main cause of long bone fractures. It indicated that about 82% of lower leg serious injuries were caused by bumper, however, 47% and 32% of thigh AIS2+ injuries were attributed to bumper and bonnet leading edge, respectively^[5].

Over past decades, many cadaver tests have been done to determine the tolerance of long bone fractures in terms of impact force and bending moment. It was reported that femur shaft fractured at peak impact forces from 3 to 10kN, and bending moments at about 320Nm^[6]. Tibia fractures were reported at peak forces from 2.5 to 8kN, and at bending moments of 280Nm for females and 320Nm for males^[4]. Most of those results are derived from 3-point bending test on long bone mid-shaft. However, the studies by Kerrigan^[7] and Ivarsson^[8] showed that response of long bone to lateral-medial bending depended significantly on loading positions. In other words, existed long bone injury criteria are controversial to assess the protect performance of designed cars since most of them were developed

according to published cadaver tests.

FE models of human body lower limb can be used to vividly show process of long bone fractures during collision and the calculated parameters like stress and strain can predict injuries based on accepted failure criteria. FE models of lower extremity were developed and validated against published cadaver tests, and then these models were used to study lower limb injury tolerance and even to assess the design of protective devices^[9-11]. However, owing to the limitations of cadaver specimens, the cadaver tests cannot truly reflect the dynamic response of lower limb. Moreover, in real car-pedestrian accidents, the injury patterns and loading conditions are more complex than those used in published literature^[12]. Therefore, accident reconstruction by using the in-depth accident investigation data is an effective method to calculate injury related parameters at varying impact conditions for evaluation of FE model^[13].

The objective of current study is to investigate the long bone fracture risk via accident reconstruction using FE model. Two pedestrian accident cases with long bone fractures were reconstructed using multi-body system model. Then a validated lower limb FE model was used to predict long bone fractures by calculating injury related parameters, such as von Mises stress and bending moment. The results are analyzed and discussed in terms of lower limb failure mechanics and injury risks.

2 METHODOLOGY AND MATERIALS

2.1 Selected accident cases

According the study of Yang^[4], about 85% of the cases the pedestrians were hit laterally, and the main accident car type was passenger car. Thus, two pedestrian cases with lower limb long bone fractures were selected in current study. The X-ray scans results were used to clarify the long bone fractures. At last, one case with detail lower leg bone fracture in GIDAS (German In-depth-Accident Study) and the other one with detail femur fracture and fibula proximal fracture in IVAC (In-depth Investigation of car accidents in Changsha) were used to conduct simulation analysis.

Case1: A car was travelling in the road with the speed of 50km/h from north to south. Suddenly, the driver found a male pedestrian was walking across the road from east to west. The driver took emergency braked with a skid mark 5~10m before the car hit the pedestrian. The pedestrian was thrown away and fell down on the ground.

Case 2: A passenger car was running near the middle line from east to west. Because it was dark and the weather was drizzle, when the driver noticed that the pedestrian was stop in front of the car, it was no time for him to take measure to avoid the accident. The driver braked emergently but still struck the pedestrian. The detail information about the cases was listed in Table 1.

2.2 Pedestrian and passenger car MBS model

Vehicle models were developed based on drawings of production cars of the same model and year as involved in the accident. The outer surface of the accident car was represented by ellipsoids. Moreover, the geometric parameters referring to the car front shape were used to control the development of car front structure^[14]. The contact stiffness of bumper used the same value in the bumper structure of the two accident cars, while the bonnet edge stiffness varied from midsection

position to side frame position due to the existence of head lamp. The stiffness characteristic curves (Fig.1) were defined using Euro-NCAP (New Car Assessment Programme) test results obtained from similar car models [15].

In current study, a 50th percentile male pedestrian dummy developed and validated by Yang et al [16] was employed as the reference dummy. The model consists of 15 ellipsoids that represent the main body parts, which are connected by 16 spherical joints. The frangible leg model in this model is used to predict the bone fracture phenomena if the impact force or bending moment exceed the tolerance level. Fig. 2 indicates the MBS car and pedestrian models using in current simulation. This model was scaled to represent the victims based on the height and weight of each involved pedestrian using the GEBOD program.

Table1 Summary of the cases information

Case No	Pedestrian			Vehicle				Injury Description	AIS
	Age	Height /cm	Mass /kg	Type	Mounting Mass/kg	Dimension L×W×H mm/mm/mm	Impact velocity /km.h ⁻¹		
1	65	174	67	Passat	1250	4580×1720×1460	37.1	Tibia shaft open fracture	3
				B3				Fibula shaft fracture	2
2	50	174	70	Jetta	1480	4385×1665×1410	26.6	Right femoral	3
				A2				intertrochanteric fracture	
								Fibula proximal fracture	2

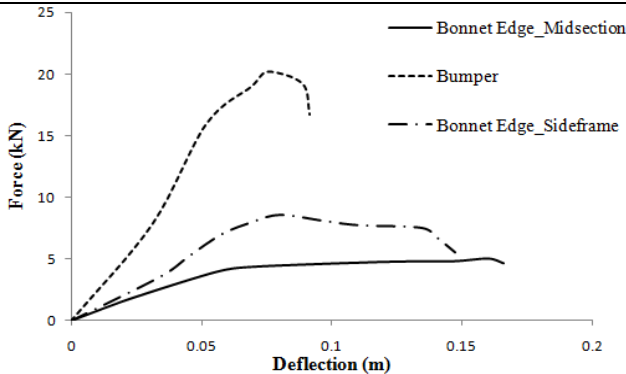


Fig.1. Contact characteristic of car front structures

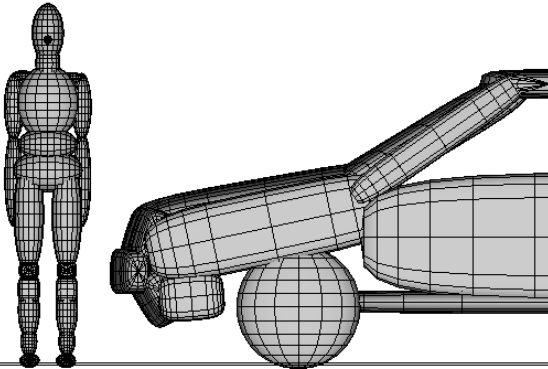


Fig.2. the baseline car-pedestrian Multi-body system model

2.3 Accident reconstruction by means of MBS method

Firstly, the code Pc-Crash was used to reproduce the accident cases in order to define the collision boundary conditions in Madymo, such as the moving speeds of accident car and pedestrian as well as

deceleration of car. The orientation and position of victim in Madymo were approximated by associating pedestrian injuries with impact points on the car. Then, parametric study was performed concerning vehicle's velocity and driving direction as well as pedestrian's speed and stance to determine the best correlations with the scene sketch from in-depth on-site investigations.

The final results agreed with the real accident record, including impact locations on the car, injuries of human and relative position between car and pedestrian at post phase of accident. These were restrained to conduct the research of next step. A friction coefficient between car and ground was considered due to the emergency brake before impact. The values of 0.6 and 0.7 from PC-Crash simulation were assigned to case1 and case2, respectively. While, the friction coefficients between pedestrian and ground as well as pedestrian body parts with car were defined as 0.6 and 0.3, respectively.

2.4 Development of FE model for lower limb injury reconstruction

The car FE model was developed based on the detail geometry of front structure of each accident car. Because the main purpose of this study is investigate the long bone fracture of lower extremity, the front structure parts involving in lower limb injury were remained, such as bumper system, head lamp, bonnet edge and bonnet. A concentrated mass node representing the car curb weight was attached at the mass gravity position to the front structure via rigid contact method. The material properties of car front structure derived from validated similar cars and adjusted according to the stiffness used in MBS car model.

The lower limb FE model used in current simulation derived from HUMOS2(Human Model for Safety) full human body model, which is developed based on European 50th percentile adult male. The lower extremity FE model was refined and validated to evaluate the performance of a bumper^[10]. In order to simulate the real accident and reproduce the friction between shoe and ground, a FE shoe was attached to this model. In addition, the pelvis was added in the original FE model to evaluate the femur proximal injuries. The ligaments and muscle around hip joint were simply represented by discrete elements. The whole model consists of 71 components and 31,205 elements. The baseline FE model for simulation of impact between car front structure and lower limb was developed and shown in Fig. 3. Considering the influence of upper body inertial force on the kinematic of lower extremity during collision, a preload of 400N was applied to the lower limb to represent the weight of upper body.

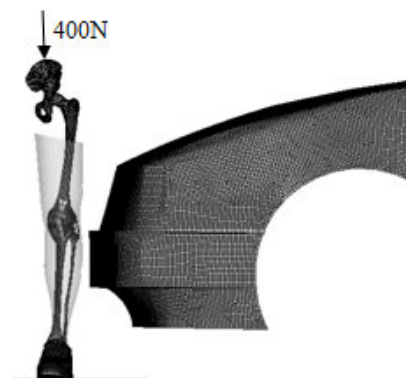


Fig.3. The baseline FE model between car front structure and lower limb

Then, the results from MBS reconstructions were used as the boundary conditions in the setup of FE simulations. Because of the differences of weight between victims and 50th percentile European

male, the preloads were adjusted to 350N and 335N in case 1 and case 2, respectively. Several sections were defined in the lower limb FE model to record the section bending moment of long bones during collisions. Long bone fractures were simulated by the elimination of elements through setting ultimate strain.

3 RESULTS

3.1 Pedestrian kinematic and rest position from MBS simulation

Fig. 4 (a) indicates the kinematics of pedestrian and the data from on-site investigation of case 1. The first impact happened between the left lower leg and the bumper, followed by the thigh impacted with bonnet leading edge at 18ms due to the inertial of upper body. Then, the upper body rotated around the bonnet leading edge, causing the head contacted with windshield at 130ms. Furthermore, the pedestrian was thrown forward and fell on the ground at 2000ms. Comparing the impact points and rest position of car and pedestrian from simulation and real record data, the simulation results have a good agreement with the in-depth on-site investigation data.

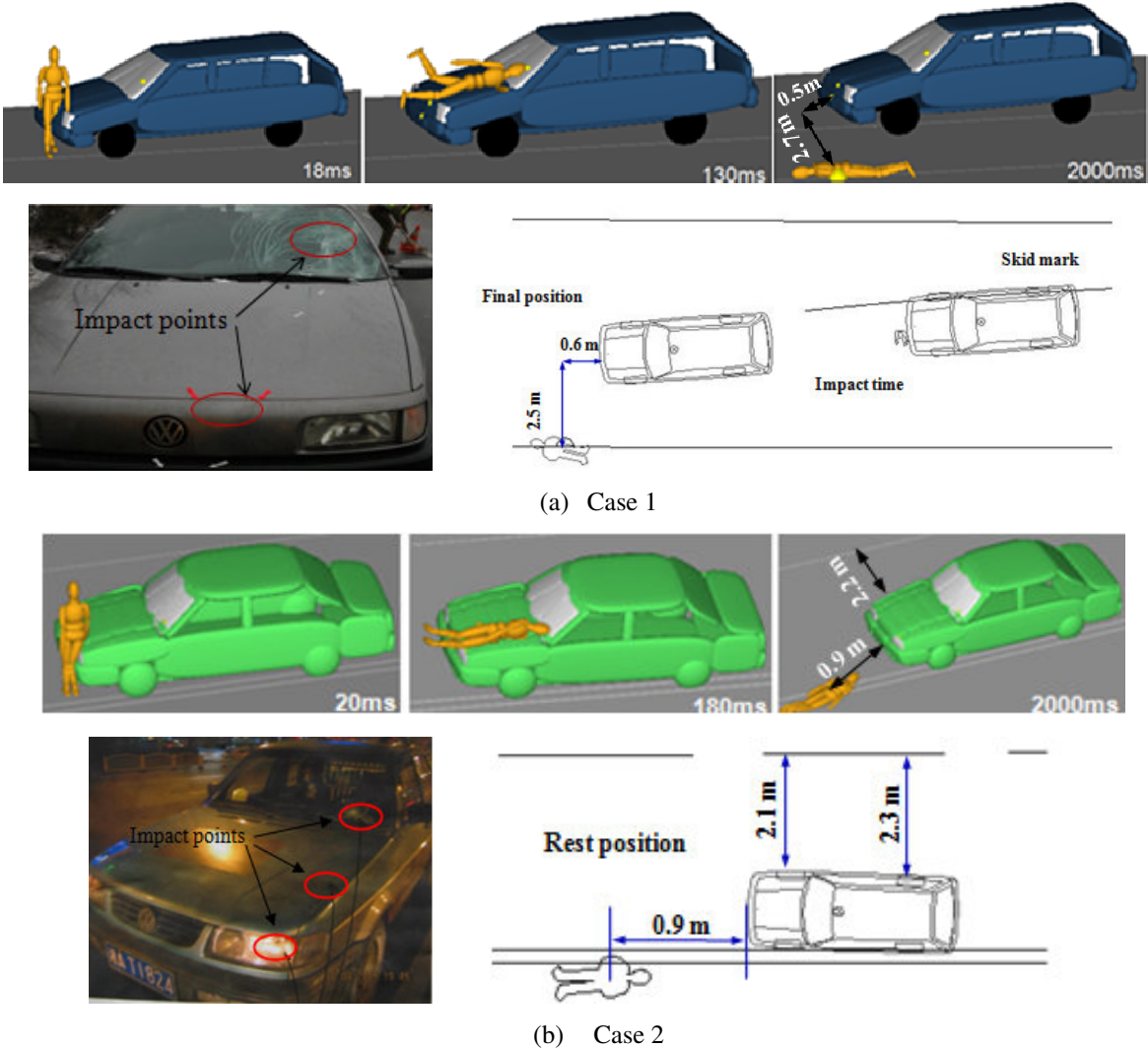


Fig.4. Pedestrian kinematics and final position comparing with real record data
 It can be seen clearly pedestrian dynamic collision process of case 2 in Fig. 4(b). The first contact

occurred between bumper and knee joint area, followed by the thigh-to-left head lamp contact at about 20ms. Furthermore, the upper body wrapped backward around car, leading the chest impacted with the rear of bonnet and head contact against windscreen at 180ms. Then, the whole body was thrown off the bonnet, fell and slid on the ground. At 2000ms, the pedestrian stopped at the final position and the simulation finished. The impact points and rest position of car and pedestrian from on-site investigation were also shown in Fig. 4(b). The reconstruction results showed good accordance with the record data from real accident through comparing the impact points and final position.

3.2 Output of kinematics from MBS reconstruction

In the MBS reconstruction, pedestrian lower limb injuries were evaluated in terms of the calculated impact force. Output impact forces and recorded injuries were compared in table2

In the case 1, the peak force in the left frangible joint reached to 5.2kN, which exceeded the reference value of 4kN. This value was set as an indicator of fracture risk of tibia. The impact force between bumper and tibia was 5.1kN, which was higher than tolerance level as well.

In case 2, the interface contact force between bumper and up section of lower leg was 3.8kN, which did not reach the tolerance of tibia but exceeded the tolerance of fibula. According to the study of Levine ^[17], the fracture force of fibula was about 0.44kN. In the simulation of case 2, pedestrian thigh proximal impacted with the bonnet leading edge and the corresponding contact force was 5kN, which indicated 20% risk of femur fracture ^[18]. The output parameters showed good agreement with the hospital record injuries in both cases.

Table 2 Comparison between output parameters and hospital record data

	Simulation	Injury Record
Case2	Bumper and up section of lower leg is 3.8kN (0.44kN as the reference fibula fracture force)	Fibular head fracture
	Bonnet leading edge and proximal femur is 5kN (indicates 20% risk of femur fracture)	Femur intertrochanteric fracture

Table 3 Initial boundary conditions for FE reconstruction

Items		vehicle		pedestrian	
		Case1	Case2	Case1	Case2
Linear velocity(m/s)	V_x	10.3	7.388	0	0
	V_y	0.72	-0.0354	1.94	0
Angular velocity(rad/s)	ω_z	0.2	-0.043	0	0

3.3 Long bone fractures predicted by FE model.

The determined velocities and orientations of pedestrians and cars from MBS reconstruction were employed as the boundary conditions in the FE model. Table 3 indicates the initial conditions for FE reconstruction. In the FE model, the process of long bone fracture was illustrated by means of output animations. Bending moments through the sections defined in the lower extremity were recorded as fracture index to evaluate the long bone injuries. Observed von Mises stress was used to clarify the long bone fracture and to detect the accuracy of long bone mechanical property as well.

The long bone fractures and recorded moment-time curves of case 1 are shown in Fig. 5 and Fig. 6,

respectively. Combining the dynamic response process and output moment, the causation and injury mechanisms of lower leg bone was identified. The pedestrian was walking and left leg was rising when the impact happened, leading the bumper firstly hit the fibular head. Flesh and skin around this region was compressed and transferred the force to fibular head at the initial impact time of 2 ms. Thus, the whole fibula bending toward the lateral direction and the moment appeared as a negative value. Then, the whole bumper contacted with the fibula and the applied force move downward to the fibula proximal, causing the fibula and tibia began to bending toward medial direction and the moment of fibula and tibia shaft was expressed by means of positive value. With the function of impact force, the bending moment of fibula and tibia increased quickly. When the tensile stress on the non-loading side reached to fracture tolerance at the time of 9 ms, tibia shaft fracture occurred. At the fracture time, recorded moment reached to 310.8 Nm and von Mises stress was 145 MPa. Then, the bending moment of fibula increased to 21.4 Nm at the time of 10 ms. Fibula fracture occurred and von Mises stress reached to 145 MPa.

Fig. 7 indicates the dynamic process of long bone fractures of case 2. The bumper first hit the knee joint region. With the function of impact force, fibular head would move toward tibia. Stress concentration occurred at the contact surface between fibular head and tibia proximal. Fibular head fracture happened when the von Mises of fibular head reached to the fracture stress of 145.4 MPa at the time of 20 ms. At the initial of collision, the impact force passed from skin and flesh to femur distal, causing the femur bending toward lateral direction and the moment of femur neck indicated minus value, as shown in Fig. 8. After the fibular head fracture, the bumper impacted the tibia component and knee joint sustained a large valgus rotation and shear displacement. Then, the femur moved toward the hood leading edge due to the inertial function of upper body. While the head lamp impacted thigh proximal, impact force employed to the femur shaft. Then, the femur began to bending toward medial direction and moment of femur neck showed positive value. Owing to the constraint of hip joint, the moment of femur neck region increased quickly until 304.7 Nm. Fracture occurred at femur neck region and the von Mises stresses of femur cortical and spongy bone reached to 137.5 MPa and 9.4 MPa, respectively.

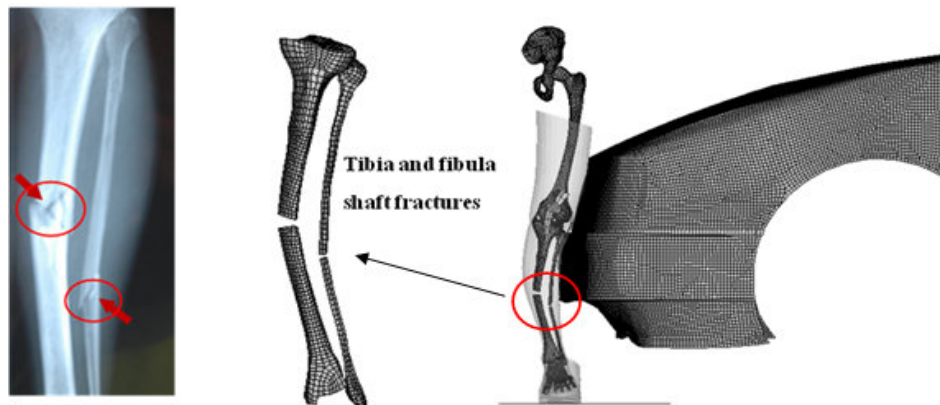


Fig.5. Comparison of long bone fractures between X-ray scanning and FE model simulation in case 1

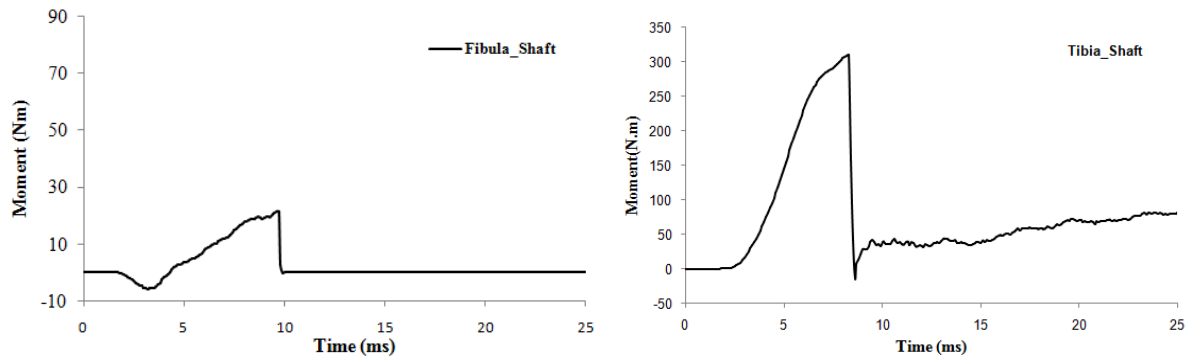


Fig.6. Moment-Time history of Fibula and Tibia from simulation of case 1

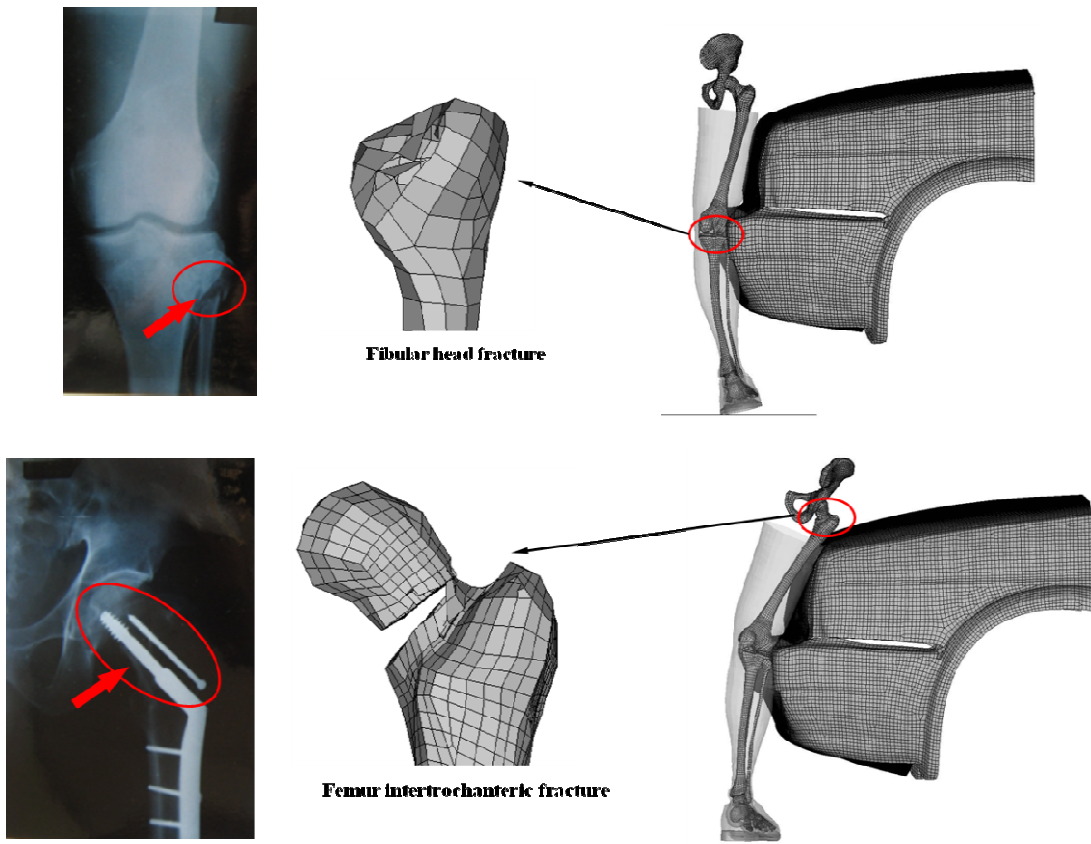


Fig.7. Comparison of long bone fractures between X-ray scanning and FE model simulation in case 2

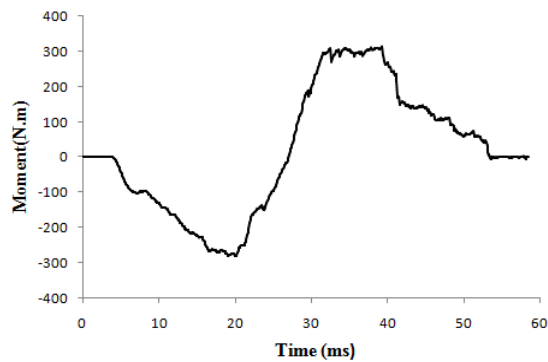


Fig.8. Moment-Time history of femoral neck from simulation of case2

4 DISCUSSION

In current study, two real-world pedestrian accidents were selected to investigate the long bone fractures which identified by X-ray scanning in hospital. The two victims were hit laterally by popular passenger car and the height of the pedestrians was closed to the height of 50th percentile European male, which represent the most common scenario of pedestrian accidents. Then, the selected cases were reconstructed through combination of MBS and FE methods.

The MBS reconstruction is able to show the human kinematic process during impact. In addition, it takes very little time to finish accident reconstruction. However, it cannot show the procedures and detail positions of lower limb injuries, which make it is difficult to indentify detailed injury mechanisms and develop injury criteria using MBS models.

The FE reconstruction can clearly show the progress and positions of long bone fractures. The dynamic response from FE model can be used to clarify the injury mechanism of long bone. Fibula proximal fracture is one common lower limb injury pattern due to the first impact usually happened between this region and bumper. In the FE injury reconstruction of case 1, it can be seen that fibula and tibia shaft fractures were attributed to bending moment caused by the impact force from bumper. In addition, tibia shaft fracture occurred before fibula shaft fracture indicates that fibula sustains more bending deflection than tibia when loading at bone shaft. Because of the restraint of knee ligaments and the friction force between shoe and ground, the dynamic responses of fibula and tibia shaft fracture process were similar to those of dynamic 3-point bending tests. Thus, to some extent the injury tolerance developed from pure tibia and fibula bending test could be considered as the injury criteria to predict long bone fracture. As indicated in case 2, the bonnet leading edge is the main reason causing femur intertrochanteric fracture. However, the fracture process of femur neck illustrates that it is not suitable to use dynamic 3-point bending tests to develop injury criteria of femur neck region.

Comparing the X-ray scans and fracture predicted by lower limb FE model, it can be seen FE model can generally reflect the fractures occurred in real world. The ultimate von Mises stress of fibula and tibia cortical predicted in the simulation is 145 MPa and the values for femur proximal cortical and cancellous are 137.5 MPa and 9.4 MPa. All the predicted ultimate von Mises stresses are in the corridor concluded by Takahashi et al ^[19]. The predicted fracture moment of fibula shaft is 21.4 Nm, which is slightly lower than the suggested fracture moment of 27 Nm ^[17]. In addition, the predicted fracture moment of tibia shaft was 310.8 Nm, which is close to the tolerance fracture at 312 Nm recommended by Kerrigan et al ^[7]. The predicted fracture moment of femur neck is 304.7 Nm. However, no available cadaver data can be used to define the tolerance of femur neck in pedestrian accident.

Information from in-depth accident investigation is very useful to validate the accuracy of reconstruction and as well as validate the biofidelity of Lower limb FE model by comparing the predicted long bone fractures and recorded injury data. It should be noticed that the fracture stress and moment obtained from simulation are only acceptable to predict long bone fractures in the same fracture locations. A large amount of pedestrian cases with different long bone fractures locations and impact conditions should be investigated and reconstructed via FE model to develop the bending strength threshold for long bones in different positions.

The disadvantage of current study is that the upper body was represented by a preload force, which cannot truly reflect the inertial function of upper body on lower extremity. In addition, it cannot simulate the mutual function between two legs. Therefore, it is necessary to develop the whole human body FE model and use the model to predict long bone fractures.

5 CONCLUSIONS

1. The lower extremity FE model has good biofidelity and can be employed to predict long bone fractures occurred in the real world accidents. It is an effective method to predict long bone fractures via reconstruction using combination of MBS and FE model. MBS method is used to reproduce the pedestrian kinematic and obtain the boundary conditions at collision. FE model is used to indicate the process and detail position of long bone fracture.
2. In-depth accident investigation is very important for the reconstruction of MBS method and validation of lower limb FE model. By comparing the long bone fractures from X-ray scanning and FE simulations, the biofidelity performance of lower limb FE model can be clarified.
3. Considering the discrepancy of specimens and boundary conditions, it is feasible to use validated FE model to predict long bone fractures. The predicted fracture moment of femoral neck is 304.7 Nm. The fracture moments for fibula and tibia shaft are 21.4 Nm and 310.8 Nm, respectively.

ACKNOWLEDGEMENTS

This study was sponsored by China Scholarship Council (CCS), and supported by Accident Research Unit of Medical University of Hannover.

REFERENCE

- [1] http://ec.europa.eu/transport/road_safety/pdf/statistics/dacota/bfs2012_dacota-intras-pedestrians.pdf
- [2] J.K. Yang, D. Otte. A Comparison Study on Vehicle Traffic Accident and Injuries of Vulnerable Road Users in China and Germany, SAE paper, No: 07-0417.
- [3] C. Untaroiu, K. Darvish, J. Crandall, et al. A finite element model of the lower limb for simulating pedestrian impacts. *Stapp Car Crash Journal*. 2005. 49:157-181.
- [4] J.K. YANG. Review of injury biomechanics in car-pedestrian collisions. *International Journal of Vehicle Safety*, 2005, 1(1-3):100-117.
- [5] Y. Mizuno. Summary of IHRA pedestrian safety WG activities (2003) – proposed test methods to evaluate pedestrian protection offered by passenger cars. The 18th International Technical Conference on the Enhanced Safety of Vehicles, Paper Number 280.
- [6] T.A. Kress, J.N. Snider, D.J. Porta, et al. Human femur response to impact loading. *Proceedings of the International IRCOBI Conference on the Biomechanics of Trauma*, September 8–10, Eindhoven, the Netherlands, 1993: 93–104.
- [7] J.R. Kerrigan, D.C. Drinkwater, C.Y. Kam, et al. Tolerance of the human leg and thigh in dynamic latero-medial bending. *International Journal of Crashworthiness*. 2004, 9(6):607-623.
- [8] B. Ivarsson, J. Kerrigan, D. Lessley, et al. Dynamic response corridors of the human thigh and leg in non-midpoint three-point bending. SAE paper. No: 2005-01-0305.
- [9] S. Kuwahara, T. Hosokawa, K. Okada, et al. Finite element analysis of pedestrian lower extremity injuries in car-to-pedestrian impacts. SAE paper. No: 2007-01-0755.
- [10] S.N. Huang, J.K. Yang, R. Fredriksson. Performance analysis of a bumper–pedestrian contact sensor system by using finite element models. *International Journal of Crashworthiness*. 2008, 13(2):149-157.
- [11] F.H. Mo, P.J. Arnoux, J.J. Jure, et al. Injury tolerance of tibia for the car–pedestrian impact. *Accident Analysis and Prevention*. 2012, 46:18-25.
- [12] Y. Han, J.K. Yang, K. Mizuno. Virtual Reconstruction of Long Bone Fracture in Car-to-pedestrian Collisions Using Multi-body System and Finite Element Method. *Chinese Journal of Mechanical Engineering*. 2011, 24(6):1045-1055.
- [13] J.K. YANG, W. XU, D. OTTE. Brain injury biomechanics in real world car accident using mathematical models. *Chinese Journal of Mechanical Engineering*, 2008, 21(4): 81–86.
- [14] J.F. Yao, J.K. Yang, D. Otte. Head Injuries in Child Pedestrian Accidents—In-Depth Case Analysis and Reconstructions *Traffic Injury Prevention*, 2007, 8(1): 94-100.
- [15] L. Martinez, L. J. GUERRA, G. Ferichola, et al. Stiffness corridors of the European fleet for pedestrian simulation. *Proceeding of the 20th International Technical Conference on the Enhanced Safety of Vehicles*, Lyon, France, 2007: No: 07-0267.

- [16] J.K. Yang, P. Lövsund, C. Cavallero, et al. A Human-body 3D mathematical model for simulation of car-pedestrian impacts. *Traffic Injury Prevention*, 2000, 2 (2): 131–149.
- [17] R. Levine. *Injuries to the Extremities*, in *Accidental Injury—Biomechanics and Prevention*. New York: Springer. 2002.
- [18] European New Car Assessment Programme. *Assessment Protocol—Pedestrian Protection*. 2009, version 5.0.
- [19] Y. Takahashi, Y. Kikuchi, A. Konosu, et al. Development and validation of the Finite Element Model for Human Lower Limb of Pedestrians. *Stapp Car Crash Journal*. 2000, 44:335-355.
- [20] G.W. Nyquist, R. Cheng, A. El-Bohy, et al. *Tibia Bending: Strength and Response*. SAE paper. No:85-1728.